Lattice Dynamics and Ionic Deformation in Some Alkali Halides*

J. S. MELVIN, J. D. PIRIE, AND T. SMITH
Department of Natural Philosophy, University of Aberdeen, Aberdeen, Scotland
(Received 27 December 1967)

Equations of motion are derived for a shell model in which the shells are allowed to deform. Dispersion curves are then calculated for NaF, NaCl, NaBr, and NaI from measured dielectric, infrared, and elastic constants. A comparison with published phonon frequencies shows that a simple model with radial deformation gives some improvement over a rigid-shell model. A rather more general treatment with increased radial deformation produces even better curves. However, the LO (0,0,1) zone-boundary phonons are not well represented by either model. The eigenvectors from the rigid-shell model and from the best deformable-shell models are then used to work out the ionic form-factor changes in NaCl when $(0,0,\eta)$ phonon states are excited, and the corresponding changes in the x-ray one-phonon cross sections along the (0,0,1) axis are obtained. It is found that the rigid-shell model gives small variations in the cross sections resulting from the displacements of the shells, and that the radial deformations give additional changes. The models predict the occurrence of asymmetries in x-ray scattering, but the intensity differences are an order of magnitude less than the effects which have been observed. Further calculations with the inclusion of deformation of the inner electrons are required.

1. INTRODUCTION

RECENTLY a discussion has been given by Buyers, Pirie, and Smith,[1] and by Smith,[2] of the x-ray scattering by phonons in a lattice composed of deformable ions. It was shown how the one-phonon cross section depends on form-factor changes resulting from the displacement of the ions from their equilibrium positions. For such a lattice the x-ray thermal scattering has an intensity variation in reciprocal space which can not be given by a lattice of rigid ions, whatever their normal mode characteristics. Such distributions have been found for NaCl (Buyers and Smith[3]), KCl (Buyers, Pirie, and Smith[1]) and for NaF (Pirie and Smith[4]), and estimates have been obtained for the corresponding changes in the form factors.

At the present time no published quantum-mechanical calculations are available for the electronic deformation from phonon excitations. Therefore these form-factor changes have been estimated using the distortions given by various versions of the shell models which can be used in discussing the dispersion curves. The form-factor changes have been obtained for the usual rigid core coupled to a rigid displaceable shell,[5-11] and also for models including radial deformation of the shell.

Section 2 contains a restatement of the particular combination of form-factor changes which can be obtained from the experimental observations, and which must be calculated from the ionic distortions. The equations of motion for the deformable shell models are derived in Sec. 3, and a discussion is given of their elastic and dielectric properties. The dispersion curves are then calculated from the measured elastic and dielectric constants, and a comparison made with published frequency measurements. Finally the eigenvectors from the models are used in Sec. 4 to obtain the form-factor changes for the $(0,0,\eta)$ phonon states.

2. RAMAN EFFECT IN PHONON SCATTERING OF X RAYS

The ionic x-ray form factors are the Fourier transforms of the charge density, which depends on the positions of neighboring ions. In Ref. 1 the form factor $f_{l\mu}$ of the μ ion in the l unit cell was taken as

$$f_{l\mu}=f_\mu(1+\sum_{l'\mu'}\beta(l-l',\mu\mu',\mathbf{K})\cdot\mathbf{x}(l',\mu')). \quad (1)$$

Here $\mathbf{x}(l',\mu')$ is the displacement of the μ' ion in the l' unit cell from its equilibrium position, and $\mathbf{K}$ is the scattering vector. It was shown that the one-phonon scattering now contains extra terms which arise from the first-order x-ray Raman effect for the vibrational levels. The one-phonon cross section is given by

$$\frac{d\sigma}{d\Omega}=\sum_{qj}\left(\frac{E}{\omega^2}\right)_{qj}\left|\sum_\mu\sum_{\mu'}f_\mu\exp(-M_\mu)\exp[i\mathbf{H}\cdot\mathbf{r}_0(0,\mu)]\times[\mathbf{K}\delta_{\mu\mu'}-i\beta(\mathbf{q},\mu\mu',\mathbf{K})]\cdot\mathbf{U}(\mu',\mathbf{q},j)\right|^2,$$

where

$$\beta_\alpha(\mathbf{q},\mu\mu',\mathbf{K})=\sum_{l'}\beta_\alpha(l-l',\mu\mu',\mathbf{K})\times\exp\{i\mathbf{q}\cdot[\mathbf{r}_0(l',\mu')-\mathbf{r}_0(l,\mu)]\},$$

$$\mathbf{K}+\mathbf{q}=\mathbf{H},$$

and $\omega(\mathbf{q},j)$ and $\mathbf{U}(\mu,\mathbf{q},j)$ are the frequency and eigenvectors of the j mode, with wave vector $\mathbf{q}$. The M_μ are the Debye-Waller exponents, and $\mathbf{r}_0(l',\mu')$ is the equi-

* Work supported in part by the Science Research Council.

[1] W. J. L. Buyers, J. D. Pirie, and T. Smith, Phys. Rev. **165**, 999 (1968).
[2] T. Smith, in *Phonons in Perfect Lattices*, edited by R. Stevenson (Oliver and Boyd, Edinburgh, 1966), p. 167.
[3] W. J. L. Buyers and T. Smith, Phys. Rev., **150**, 758 (1966).
[4] J. D. Pirie and T. Smith, J. Phys. C**1**, 648 (1968).
[5] B. J. Dick and A. W. Overhauser, Phys. Rev. **112**, 90 (1958).
[6] J. E. Hanlon and A. W. Lawson, Phys. Rev. **113**, 472 (1959).
[7] W. Cochran, Phys. Rev. Letters **2**, 495 (1959).
[8] W. Cochran, Proc. Roy. Soc. (London) **A253**, 260 (1959).
[9] A. D. B. Woods, W. Cochran, and B. N. Brockhouse, Phys. Rev. **119**, 980 (1960).
[10] R. A. Cowley, W. Cochran, B. N. Brockhouse, and A. D. B. Woods, Phys. Rev. **131**, 1030 (1963).
[11] R. A. Cowley, Proc. Phys. Soc. (London) **A268**, 109 (1962).

librium position of the l',μ' nucleus. In general $\beta(l-l', \mu\mu', \mathbf{K})$ and $\beta(\mathbf{q},\mu\mu',\mathbf{K})$ are complex. The one-phonon cross sections at equivalent points ($\mathbf{K}=\mathbf{H}\pm\mathbf{q}$) on either side of a Bragg peak with reciprocal lattice vector $\mathbf{H}$ are of particular interest. They will be changed in different senses if $\beta(\mathbf{q},\mu\mu',\mathbf{K})$ reverses sign when $\mathbf{q}$ is replaced by $-\mathbf{q}$. These changes will be equal in magnitude if $\beta(\mathbf{q},\mu\mu',\mathbf{K})$ is independent of $\mathbf{K}$. Asymmetries in the intensities of this character have been observed in the alkali halides.[1-4] If, on the other hand, $\beta(\mathbf{q},\mu\mu',\mathbf{K})$ is an even function of $\mathbf{q}$, the shifts in the two intensities will be in the same sense. The even or odd character of $\beta(\mathbf{q},\mu\mu',\mathbf{K})$ is determined by the sign relation between $\beta(l-l', \mu\mu', \mathbf{K})$ and $\beta(l'-l, \mu\mu', \mathbf{K})$ and so depends on the character of the distortion. If the $\mathbf{K}$ dependence is small, it can be shown that shell displacements lead to shifts and radial distortions give asymmetries.

3. IONIC DISTORTION AND PHONON DISPERSION

A. Rigid-Shell Model

The distortion considered in the shell model[5-11] is the displacement of a rigid shell of charge with respect to a rigid core formed by the nucleus and the inner tightly bound electrons. The derivation of the equations of motion will be indicated in this section because the introduction of shell deformation (Sec. 3 B) forms an extension of the formalism.

In the harmonic approximation the equation of motion of the l,μ core or shell is

$$m_\mu \ddot{x}(l,\mu,\alpha) = -\sum_{l'\mu'\beta} \phi_{\alpha\beta}(ll',\mu\mu')x(l',\mu',\beta), \qquad (2)$$

where $-\phi_{\alpha\beta}(ll',\mu\mu')$ is the Born–von Karman coefficient giving the force in the α direction on the l,μ shell or core when l',μ' is displaced in the β direction. For a particular mode,

$$\mathbf{m}_c\omega^2\mathbf{U}=\mathbf{N}\mathbf{U}+\mathbf{H}\mathbf{V},$$
$$\mathbf{m}_s\omega^2\mathbf{V}=\mathbf{H}^\dagger\mathbf{U}+\mathbf{E}\mathbf{V},$$

where $\mathbf{U}$ and $\mathbf{V}$ are the core and shell eigenvectors, and $\mathbf{m}_c$ $\mathbf{m}_s$ are diagonal matrices containing the core and shell masses, respectively. The interactions have been grouped so that the matrix $\mathbf{N}$ describes all core-core, $\mathbf{H}$ all core-shell, and $\mathbf{E}$ all shell-shell suitably phased forces. A typical element of one of these matrices is

$$N_{\alpha\beta}=\sum_{l'} \phi_{\alpha\beta}{}^c(ll',\mu\mu') \exp\{i\mathbf{q}\cdot[\mathbf{r}_0(l',\mu')-\mathbf{r}_0(l,\mu)]\}.$$

The matrices $\mathbf{N}$, $\mathbf{H}$, and $\mathbf{E}$ can be further split to show the different classes of force. Thus, the core-core matrix $\mathbf{N}$ can be given in terms of the Kellerman coefficients $\mathbf{C}$ for the long-range Coulomb forces, the core-shell forces $\mathbf{k}$, and the short-range coupling with any number of neighboring cores $\mathbf{I}$. The elements of $\mathbf{I}$ are functions of $\mathbf{q}$ and combinations of the Born–von Karman coefficients of Eq. (2). $\mathbf{I}$ is shown schematically along with

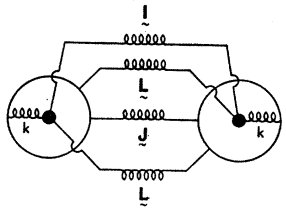

FIG. 1. Schematic forces between neighboring ions in the shell model.

the other similar force groupings $\mathbf{L}$ and $\mathbf{J}$ in Fig. 1. The equations of motion in the adiabatic approximation can then be written as

$$\begin{aligned}\mathbf{m}_c\omega^2\mathbf{U}&=(\mathbf{I}+\mathbf{X}\mathbf{C}\mathbf{X}+\mathbf{k})\mathbf{U}+(\mathbf{L}+\mathbf{X}\mathbf{C}\mathbf{Y}-\mathbf{k})\mathbf{V},\\ 0&=(\mathbf{L}^\dagger+\mathbf{Y}\mathbf{C}^\dagger\mathbf{X}-\mathbf{k})\mathbf{U}+(\mathbf{J}+\mathbf{Y}\mathbf{C}\mathbf{Y}+\mathbf{k})\mathbf{V},\end{aligned} \qquad (3)$$

where $\mathbf{X}$, $\mathbf{Y}$, and $\mathbf{Z}$ are diagonal matrices giving the charges on the cores, shells, and ions, respectively. The relative displacement of shell and core for each ion $\mathbf{W}=\mathbf{V}-\mathbf{U}$ may be obtained from

$$\begin{aligned}\mathbf{m}_c\omega^2\mathbf{U}&=(\mathbf{I}+\mathbf{L}+\mathbf{L}^\dagger+\mathbf{J}+\mathbf{Z}\mathbf{C}\mathbf{Z})\mathbf{U}+(\mathbf{L}+\mathbf{J}+\mathbf{Z}\mathbf{C}\mathbf{Y})\mathbf{W},\\ 0&=(\mathbf{L}+\mathbf{J}+\mathbf{Z}\mathbf{C}\mathbf{Y})^\dagger\mathbf{U}+(\mathbf{J}+\mathbf{Y}\mathbf{C}\mathbf{Y}+\mathbf{k})\mathbf{W},\end{aligned}$$

by first expressing $\mathbf{W}$ in terms of $\mathbf{U}$ to give an effective dynamical force matrix between the cores, and diagonalizing to obtain the eigenvectors $\mathbf{U}$.

The Born–von Karman coefficients of Eq. (2) can be used to define A, $A(1)$, $A(2)$; B, $B(1)$, $B(2)$, and B'' in a similar way to Woods, Cochran, and Brockhouse.[9] With these definitions A corresponds to a bond stretching force for a nearest-neighbor pair, and $A(2)$, $A(1)$ are the stretching constants for next-nearest-neighbor anion-anion and cation-cation pairs. B, $B(2)$, and $B(1)$ are the corresponding parameters for the tangential forces, and any noncentral force between nearest neighbors is represented by the force constant B''. This nomenclature is used in subsequent sections.

B. Deformable-Shell Models

More general deformations than those described by the displacement of a rigid shell may be introduced in a number of different ways. Quadratic and higher terms in the deformation can be considered[11]; however, it is not then possible to determine the coefficients from the macroscopic data. Whenever extra degrees of freedom are introduced into the dynamical system, the changes in the equations of motion can be obtained from the extra Born–von Karman coefficients. The specific modification considered here is that the radius of each shell is variable. This can be regarded as giving some account of quadrupole effects, because the quadrupole moments of the shells change linearly with the radii $r(l,\mu)$. An unmanageable number of extra parameters is not required.

Since the rigid-shell model is normally used with the short-range interactions between nearest-neighbor and next-nearest-neighbor ions, acting only between the

shells, the inclusion of radial deformation will be discussed with the same limitation. The more general expressions can be easily obtained. The extra coupling which results from the radial degrees of freedom are specified by extra Born–von Karman coefficients. In this way the equations of motion and the relations to the macroscopic constants can be obtained without any discussion of the relation of the coefficients to a particular model.

The new coefficients transform under rotation as covarient tensors of rank 1; thus for a typical nearest-neighbor pair only five are nonzero when each atomic site has cubic symmetry. If l',μ' is the nearest-neighbor ion in the x direction to the l,μ ion, then the new coefficients define ϵ parameters for this ion pair

$$\begin{aligned}\partial^2\phi/\partial x(l,\mu)\partial r(l',\mu') &= \epsilon_\mu A e^2/2v,\\ \partial^2\phi/\partial r(l,\mu)\partial r(l',\mu') &= \epsilon_{\mu\mu'} A e^2/2v,\\ \partial^2\phi/\partial r^2(l,\mu) &= \epsilon_{\mu\mu} e^2/v,\end{aligned} \tag{4}$$

in which $\mu,\mu'=1,2$; $\mu\neq\mu'$. A schematic representation is given in Fig. 2. For the next-nearest-neighbor pairs, the most important extra coefficient is the radial translational coupling between the ions. This can be adequately specified by one parameter for each ion type:

$$\partial^2\phi/\partial x(l\mu)\partial r(l'\mu) = \epsilon_\mu' A(\mu) e^2/2v.$$

The constants A and $A(\mu)$ are obtained from the Born–von Karman coefficients as in Sec. 2 A. The coefficients for all the symmetry related nearest neighbors and next-nearest neighbors may now be obtained in the usual way so that the new terms in the dynamical matrix can be found. For example, the extra coefficients for atoms related by the inversion operator are equal in magnitude but opposite in sign. Thus the matrix element coupling radial motion of the shell of type μ to the translational motion in the x direction of all the nearest-neighbor shells is

$$\epsilon_\mu A(e^2/2v)[\exp(iq_xa)-\exp(-iq_xa)] = i\epsilon_\mu A(e^2/v)\sin q_xa,$$

where a is the nearest-neighbor distance.

By similar arguments it can be shown that the equations of motion for the deformable shell with both ions polarizable are

$$\mathbf{m}_c\omega^2\mathbf{U} = (\mathbf{I}+\mathbf{XCX}+\mathbf{k})\mathbf{U}+(\mathbf{L}+\mathbf{XCY}-\mathbf{k})\mathbf{V}, \tag{5a}$$

$$\mathbf{0} = (\mathbf{L}+\mathbf{XCY}-\mathbf{k})^\dagger\mathbf{U}+(\mathbf{J}+\mathbf{YCY}+\mathbf{k})\mathbf{V}+\mathbf{S}_R{}^V, \tag{5b}$$

$$\begin{aligned}0 = {}&\mathbf{S}^\dagger(2)\cdot\mathbf{V}(2)+\mathbf{S}'^\dagger(1)\cdot\mathbf{V}(1)\\ &+Q(1,1)R(1)+Q(1,2)R(2),\end{aligned} \tag{5c}$$

$$\begin{aligned}\mathbf{0} = {}&\mathbf{S}^\dagger(1)\cdot\mathbf{V}(1)+\mathbf{S}'^\dagger(2)\cdot v(2)\\ &+Q(1,2)R(1)+Q(2,2)R(2),\end{aligned} \tag{5d}$$

where

$$Q(ij) = \epsilon_{ii}\delta_{ij}+\epsilon_{12}A(c_x+c_y+c_z)(1-\delta_{ij}) \tag{6}$$

with the radial self-force constants as the diagonal elements,

$$\mathbf{S}_R{}^V = \left(\begin{bmatrix}\mathbf{S}(1)R(2)\\ \mathbf{S}(2)R(1)\end{bmatrix}+\begin{bmatrix}\mathbf{S}'(1)R(1)\\ \mathbf{S}'(2)R(2)\end{bmatrix}\right)\frac{e^2}{v},$$

where

$$\begin{aligned}\{S(\mu)\}_x &= i\epsilon_\mu A S_x,\\ \{\mathbf{S}'(\mu)\}_x &= i\epsilon_\mu' A(\mu) S_x(C_y+C_z),\end{aligned}$$

and

$$\begin{aligned}C_x &= \cos q_xa,\\ S_x &= \sin q_xa.\end{aligned}$$

Equations (5c) and (5d) now give $R(1)$ and $R(2)$ in terms of shell displacements:

$$\begin{aligned}R(1) = {}&[\alpha_1\mathbf{S}'^\dagger(1)+\beta_1\mathbf{S}^\dagger(1)]\cdot\mathbf{V}(1)\\ &+[\alpha_1\mathbf{S}^\dagger(2)+\beta_1\mathbf{S}'^\dagger(2)]\cdot\mathbf{V}(2),\end{aligned} \tag{7}$$

$$\begin{aligned}R(2) = {}&[\alpha_2\mathbf{S}'^\dagger(1)+\beta_2\mathbf{S}^\dagger(1)]\cdot\mathbf{V}(1)\\ &+[\alpha_2\mathbf{S}^\dagger(2)+\beta_2\mathbf{S}^\dagger(2)]\cdot\mathbf{V}(2),\end{aligned}$$

where

$$\alpha_1 = Q(2,2)/\det Q, \quad \alpha_2=\beta_1=-Q(1,2)/\det Q,$$

and

$$\beta_2 = Q(1,1)/\det Q.$$

In this situation the modified coupling between the translational motion of the shells can be described by a matrix $\mathbf{D}_R{}^S$ defined by

$$\mathbf{S}_R{}^V = \mathbf{D}_R{}^S\mathbf{V} = (\mathbf{D}_R{}^S(1)+\mathbf{D}_R{}^S(2))\mathbf{V}, \tag{8}$$

where

$$\mathbf{D}_R{}^S(1) = \begin{bmatrix}\beta_1\mathbf{S}(1)\mathbf{S}'^\dagger(1)+\beta_2\mathbf{S}(1)\mathbf{S}^\dagger(1) & \beta_1\mathbf{S}(1)\mathbf{S}^\dagger(2)+\beta_2\mathbf{S}(1)\mathbf{S}'^\dagger(2)\\ \alpha_1\mathbf{S}(2)\mathbf{S}'^\dagger(1)+\beta_1\mathbf{S}(2)\mathbf{S}^\dagger(1) & \alpha_2\mathbf{S}'(2)\mathbf{S}^\dagger(2)+\beta_1\mathbf{S}(2)\mathbf{S}'^\dagger(2)\end{bmatrix}\frac{e^2}{v}$$

and

$$\mathbf{D}_R{}^S(2) = \begin{bmatrix}\alpha_1\mathbf{S}'(1)\mathbf{S}'^\dagger(1)+\beta_1\mathbf{S}'(1)\mathbf{S}^\dagger(1) & \alpha_1\mathbf{S}'(1)\mathbf{S}^\dagger(2)+\beta_1\mathbf{S}'(1)\mathbf{S}'^\dagger(2)\\ \beta_1\mathbf{S}(2)\mathbf{S}'^\dagger(1)+\beta_2\mathbf{S}'(2)\mathbf{S}^\dagger(1) & \beta_1\mathbf{S}'(2)\mathbf{S}^\dagger(2)+\beta_2\mathbf{S}'(2)\mathbf{S}'^\dagger(2)\end{bmatrix}\frac{e^2}{v}.$$

A comparison with the rigid-shell equations [Eq. (3)] shows that the effect of radial deformations on the translational motion can be obtained by replacing $\mathbf{J}$ by $\mathbf{J}+\mathbf{D}_R{}^S$.

In the simple situation of only the negative ion polarizable and with the extra short-range interaction restricted to nearest neighbors, the effective dynamical matrix for the nuclei $\mathbf{D}(\mathbf{q})$ is related to the matrix for the corresponding rigid-shell model $\mathbf{D}_{\mathrm{RSM}}(\mathbf{q})$ by

$$\mathbf{D}(\mathbf{q}) = \mathbf{D}_{\mathrm{RSM}}(\mathbf{q})+\gamma\mathbf{D}_R(\mathbf{q}),$$

where $\mathbf{D}_R(q) = \sin q_\alpha a \sin q_\beta a$, with $\alpha,\beta\leq 3$,

$$= 0 \quad \text{otherwise},$$

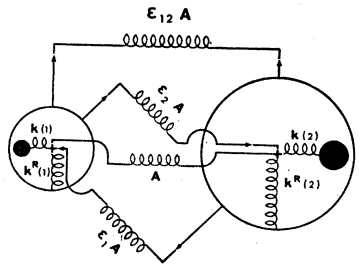

FIG. 2. Schematic forces between neighboring ions in the deformable-shell model.

and

$$\gamma=-\frac{(\epsilon_1 A)^2}{\epsilon_{11}}\frac{e^2}{v}. \tag{9}$$

Thus the changes in the dispersion curves due to radial deformation depend not on the individual parameters, but on γ, which can be obtained from the elastic constants (Sec. 3 C). When next-nearest-neighbor interactions are included in their simplest form, that is, between rigid ions, then the dispersion curves depend on A,$A(2)$, B,$B(2)$, B'', $k(2)$, Y, and γ. These cannot all be determined from the elastic and dielectric macroscopic data (Sec. 3 C). However the values of the parameters, or relations between the parameters, can be obtained if specific model assumptions regarding the potential energy ϕ are made. For example, the potential energy for the interaction between a pair of shells can be taken as depending only on the shortest distance between the shells;

$$\phi(ll',\mu\mu')=\phi(|\mathbf{x}(l',\mu')-\mathbf{x}(l,\mu)-r(l',\mu')-r(l,\mu)|). \tag{10}$$

This would correspond to the shell-shell forces localized in the bond regions. The short-range potential then contains a contribution from a sum of such terms,

$$\phi^S=\sum_{l'\mu'}\phi(ll',\mu\mu');$$

ϵ_μ and $\epsilon_{\mu\mu'}$ for $\mu\neq\mu'$ depend only on this contribution. From Eq. (4) it can be easily shown that for this model $\epsilon_\mu=\epsilon_{\mu\mu'}=1$ for $\mu\neq\mu'$. The parameters $\epsilon_{\mu\mu}$ also occur in the equations of motion. They describe the self-force appropriate to a radial expansion of shell type μ, so that ϕ^S contributes to these derivatives. The remaining contributions come from the core-shell forces within an ion and also from the intrashell forces. The derivatives of this contribution will be called $k^r(\mu)$. Thus the total model potential gives

$$\epsilon_{\mu\mu}=3A+k^r(\mu).$$

In special situations it may not be necessary to determine $\epsilon_{\mu\mu}$ separately from the macroscopic data, since it may be related, through $k^r(\mu)$, to $k(\mu)$ describing the core-shell force. Thus if the intrashell forces are small, and if the coupling is uniform between the shell surface and the core, it can easily be shown that $k^r(\mu)=3k(\mu)$. Different model assumptions regarding the core-shell and intrashell forces will give different relations between $k(\mu)$ and $k^r(\mu)$. In some circumstances these can be separately fixed from the macroscopic data.

Schröder and co-workers[12,13] have discussed radial deformation in a shell model. The equations of motion obtained[13] are similar in form to those in Eq. (5) with $\epsilon_\mu=\epsilon_{\mu\mu'}=1$ and $\epsilon_{\mu\mu}=3A+k(\mu)$.

The discussion in the rest of this paper will be restricted to rigid positive ions and to short-range next-nearest-neighbor interactions only between the negative ions. Two sets of dispersion curves with one ion polarizable and with radial deformation are given in Sec. 3 D. The first set uses the relation $k^r=3k$ together with all the nearest-neighbor values of ϵ taken as unity and the next-nearest-neighbor values taken as zero. This will be called the simple deformable-shell model. The second model will be called the deformable-shell model, and here no relation is assumed between k and k^r, but the same values of ϵ are used.

Calculations with both ions polarizable have been made in a similar way to those given in Sec. 3 D, but the dispersion curves for both rigid and deformable shells obtained from the macroscopic data give less satisfactory agreement with phonon measurements.

C. Elastic and Dielectric Constants with Radial Deformation

The dielectric and elastic properties with radial deformation can be obtained from the solutions of the equations of motion for small wave vectors. The deformable-shell equations for the optic modes in this limit are identical with those for a rigid shell, so the Lyddane-Sachs-Teller[14] relation remains valid. Equations (11)–(14) between ω_{T0} the dielectric constants and the parameters are also unchanged for the same reasons.

$$\omega_{T0}^2=\frac{4\pi}{9\mu}\frac{[(\epsilon_\infty+2)(z-d)]^2}{\epsilon_0-\epsilon_\infty}\frac{e^2}{v}, \tag{11}$$

with

$$\mu=\frac{m_1m_2}{m_1+m_2},\quad d=\frac{-S_0Y}{S_0+k}$$

and

$$S_0=A+2(B+B'').$$

$$\alpha_\infty=\frac{3}{4\pi}\frac{\epsilon_\infty-1}{\epsilon_\infty+2}=\frac{Y^2}{S_0+k}, \tag{12}$$

$$\frac{\alpha_0-\alpha_\infty}{\alpha_\infty}=\frac{(z-d)^2}{S_0\alpha_\infty-d^2}, \tag{13}$$

$$B+2B(2)=-\tfrac{2}{3}\alpha_m Z^2. \tag{14}$$

[12] U. Schröder, Solid State Commun. 4, 347 (1966).
[13] V. Nüsslein and U. Schröder, Phys. Status Solidi 21, 309 (1967).
[14] R. Lyddane, R. Sachs, and E. Teller, Phys. Rev. 59, 673 (1941).

TABLE I. Model parameters calculated from macroscopic data.

	NaI			NaBr			NaCl			NaF		
	Rigid shell	Simple deformable shell	Deformable shell	Rigid shell	Simple deformable shell	Deformable shell	Rigid shell	Simple deformable shell	Deformable shell	Rigid shell	Simple deformable shell	Deformable shell
$Y(e)$	2.67	2.67	2.67	2.96	2.96	2.96	2.67	2.67	2.67	2.25	2.25	2.25
$k(e^2/v)$	67.9	67.9	67.9	97.0	97.0	97.0	90.0	90.0	90.0	98.8	98.8	98.8
$\gamma(e^2/v)$	0	−0.582	−1.54	0	−0.380	−1.10	0	−0.38	−1.09	0	−0.349	−1.02
$A(e^2/2v)$	11.6	11.8	12.1	10.8	11.1	11.2	10.6	10.7	11.0	10.4	10.7	10.7
$A1(e^2/2v)$	0	0	0	0	0	0	0	0	0	0	0	0
$A2(e^2/2v)$	0.063	0.55	1.41	−0.035	0.76	0.89	−0.12	0.20	0.83	−0.44	0.28	0.41
$B1(e^2/2v)$	0	0	0	0	0	0	0	0	0	0	0	0
$B2(e^2/2v)$	0.052	−0.045	−0.22	−0.12	−0.28	−0.31	−0.071	−0.135	−0.26	−0.034	−0.18	−0.20
$B''(e^2/2v)$	0.017	−0.28	−0.79	−0.069	−0.54	−0.63	0.0054	−0.184	−0.56	0.0025	−0.432	−0.51

TABLE II. Input data for model calculations.

Substance	Phonon frequencies	a(Å)	c_{11} (10^{-12} dyn/cm^2)	c_{12} (10^{-12} dyn/cm^2)	c_{44} (10^{-12} dyn/cm^2)	ω_0 (10^{-12} radians/sec)	ϵ_0	ϵ_∞
NaI	16	3.21[a]	0.359[a]	0.075[a]	0.0768[a]	22.8[a]	6.18[a]	2.91[a]
NaBr	17	2.987[b]	0.401[c]	0.109[c]	0.099[c]	25.45[d]	6.38[d]	2.60[e]
NaCl	18	2.81[b]	0.488[f]	0.126[f]	0.127[f]	30.9[d]	5.91[d]	2.31[d]
NaF	19	2.312[b]	0.971[g]	0.243[g]	0.280[g]	46.4[h]	5.1[i]	1.739[e]

[a] Reference 9. [b] Reference 15. [c] Reference 16. [d] Reference 17. [e] Reference 18. [f] Reference 19. [g] Reference 20. [h] Reference 21. [i] Reference 22.

Here α_m is the Madelung constant and α_∞ and α_0 are the high- and low-frequency crystal polarizabilities. These relations are used in fixing the parameters in Sec. 3D. In a similar way, relations between the parameters and the elastic constants can be obtained from the ω/q ratio for the acoustic modes at small values of q. The elastic constants can always be expressed in terms of the elements of the dynamical matrix in a way which is independent of the model. Thus Woods, Cochran, and Brockhouse[9] show that to a scale factor

$$c_{11}=D_2(1,1)+D_2(4,4)+2D_2(1,4) \quad \text{for} \quad q=(q_x,0,0),$$
$$c_{44}=D_2(2,2)+D_2(5\,5)+2D_2(2,5) \quad \text{for} \quad q=(q_x,0,0),$$
$$\tfrac{1}{2}(c_{11}-c_{12})=D_2(1,1)-D_2(1,2)+D_2(4,4)-D_2(4,5)+2[D_2(1,4)-D_2(1,5)] \quad \text{for} \quad q=(q_x,q_y,0),$$

where $D_2(ij)$ is the coefficient of q^2 in a power-series expansion of the (i,j) element of the dynamical matrix. Substitution of the coefficients for the deformable-shell model gives

$$\begin{aligned} c_{11}&=-5.110Z^2+A+A(2)+B(2)+\gamma,\\ c_{44}&=1.391Z^2+\tfrac{1}{2}[A(2)-B(2)]+B'', \qquad (15)\\ c_{12}&=1.391Z^2+\tfrac{1}{2}[A(2)-B(2)]-B''+\gamma, \end{aligned}$$

where the elastic constants are given in units of $e^2/4a^4$ and A, $A(2)B(2)$, B'', and γ are as defined in Sec. 3 A. Since the corresponding equations for a rigid shell are obtained with $\gamma=0$, it is clear that the relation between the parameters and the elastic constants are changed if radial deformation is allowed. With radial deformation it also follows from these equations that even if the forces are central in character ($B''=0$), then the γ term ensures that the Cauchy relation ($C_{12}=C_{44}$) will not be obeyed.

It seems that some of the numerical values for the parameters used by Schröder and co-workers[12,13] in calculating dispersion curves with radial deformation were obtained from the macroscopic data by the relations appropriate to a rigid shell, rather than by the relations given above.

D. Model Calculations

The effect of incorporating radial deformation in NaI, NaBr, NaCl, and NaF has been obtained by calculating the phonon-dispersion curves along the principal symmetry directions for both the simple deformable shell and for the deformable-shell models. The model parameters are given in Table I and the macroscopic data from which they are determined are shown in Table II.[15–22]

[15] R. W. G. Wyckoff, *Crystal Structures* (Interscience Publishers, Inc., New York, 1964), Vol. 1.
[16] R. P. Lowndes, Phys. Letters **21**, 26 (1966).
[17] D. H. Martin, Advan. Phys. **14**, 39 (1965).
[18] J. Tessman, A. Kahn, and W. Schockley, Phys. Rev. **92**, 890 (1953).
[19] J. T. Lewis, A. Lehoczky, and C. V. Briscoe, Bull. Am. Phys. Soc. **10**, 44 (1965).
[20] K. Spangenberg and S. Haushaul, Z. Krist. **109**, 436 (1957).
[21] M. Born and K. Huang, *Dynamical Theory of Crystal Lattices* (Oxford University Press, Oxford, England, 1954).
[22] S. Haushaul, Z. Naturforsch. **129**, 445 (1957).

TABLE III. Values of the magnitude $\beta(\mathbf{q},\mu\mu',\mathbf{K})$ for NaCl as calculated from a rigid-shell model using the three charge distributions (a), (b), and (c). All quantities are in units of $\pi/10a$. (Cation $\mu=1$; anion $\mu=2$).

Scattering vector K	$\beta(\mathbf{q},21,\mathbf{K})$ (a)	(b)	(c)	$\beta(\mathbf{q},22,\mathbf{K})$ (a)	(b)	(c)
(0,0, 3.8)	0.10	−0.54	−0.23	−0.10	0.53	0.23
(0,0, 4.2)	0.015	−0.63	−0.14	−0.01	0.63	0.14
(0,0, 3.6)	0.14	−0.45	−0.26	−0.13	0.43	0.24
(0,0, 4.4)	−0.016	−0.64	−0.084	0.015	0.61	0.076
(0,0, 3.4)	0.19	−0.34	−0.27	−0.18	0.32	0.22
(0,0, 4.6)	−0.035	−0.61	−0.02	0.031	0.56	0.018
(0,0, 3.2)	0.31	−0.23	−0.27	−0.26	0.20	0.20
(0,0, 4.8)	−0.038	−0.56	0.043	0.032	0.48	−0.032
(0,0, 3.0)	0.35	−0.11	−0.25	−0.30	0.093	0.17
(0,0, 5.0)	−0.038	−0.47	0.12	0.032	0.39	−0.084

For the short-range interactions restricted to nearest neighbors, the shell distortion is entirely determined by γ from (see Sec. 3 C).

$$\gamma=(4a_0^4/e^2)(c_{44}+c_{12})-2.782Z^2.$$

As expected from Eq. (9), all the crystals have negative values for γ (Table I). The dispersion curves give some improvement over the corresponding rigid-shell predictions. Thus for NaBr [23] the value of χ^2 decreases from 18.4 to 17.3.

$$\chi^2=\sum_{i=1}^{N}\frac{(\nu_{i\text{calc}}{}^2-\nu_{i\text{meas}}{}^2)^2}{4\nu_{i\text{meas}}{}^2\sigma^2(\nu_i)}\frac{1}{N},$$

where $\sigma(\nu_i)$ is the standard deviation in the neutron frequency measurement. However, since all nearest-neighbor models give comparatively poor predictions, the detailed dispersion curves are not shown here. It may be noted that when the value of γ is positive,

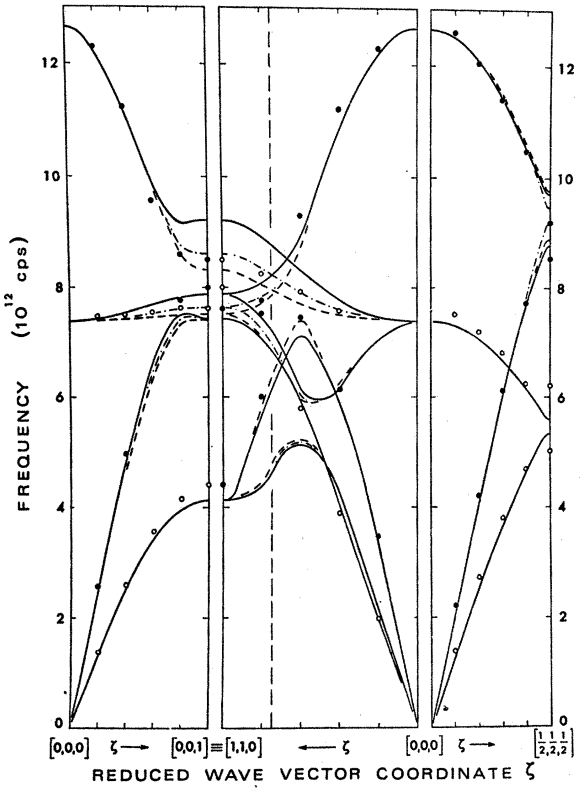

FIG. 3. Dispersion curves for NaF. Shell model (dash), simple deformable shell (dash-dot), deformable shell (solid), and experimental frequency (dot) (Buyers, Ref. 24).

[23] J. S. Reid, T. Smith, W. J. L. Buyers, and G. C. Peterson (to be published).

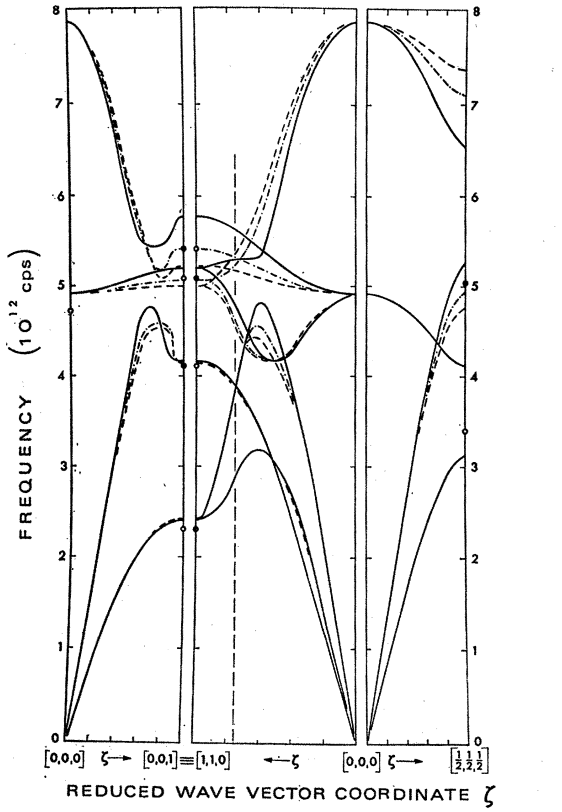

FIG. 4. Dispersion curves for NaCl. Shell model (dash), simple deformable shell (dash-dot), deformable shell (solid), and experimental frequency (dot) (Shmunk, Ref. 25).

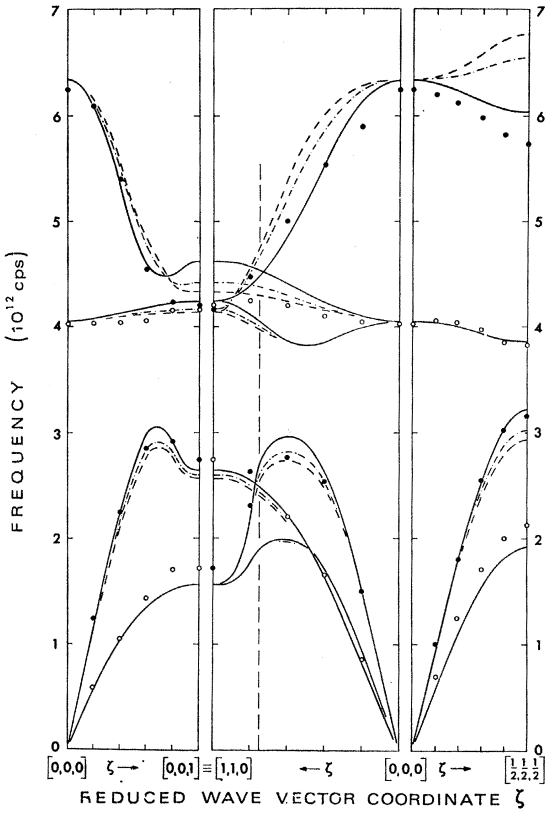

FIG. 5. Dispersion curves for NaBr. Shell model (dash), simple deformable shell (dash-dot), deformable shell (solid), and experimental frequency (dot) (Reid *et al.*, Ref. 23).

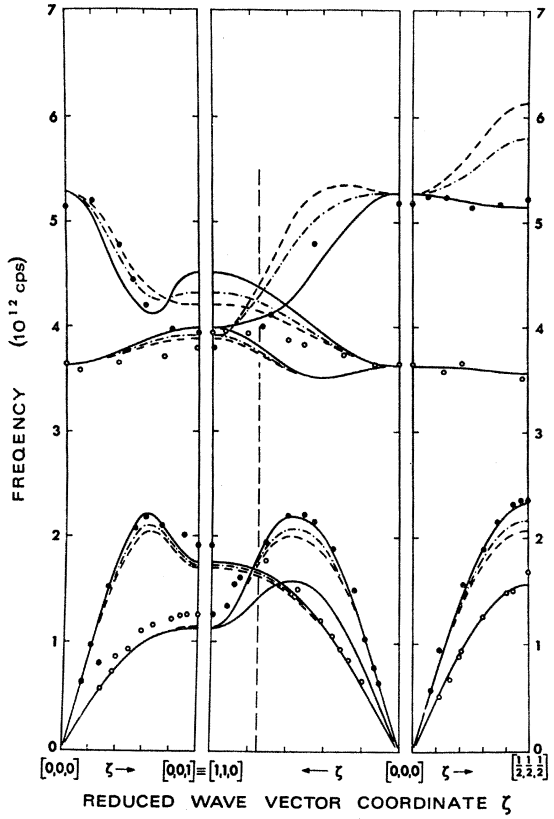

FIG. 6. Dispersion curves for NaI. Shell model (dash), simple deformable shell (dash-dot), deformable shell (solid), and experimental frequency (dot) (Woods *et al.*, Ref. 26).

as for LiF, then radial deformation in a nearest-neighbor model would be expected to lead to a less satisfactory account of the phonon frequencies than a rigid shell. Also, when a particularly large negative value of γ is obtained, as with MgO, then the radial deformation gives a large improvement in the dispersion curves.

It is only when next-nearest-neighbor models are used that good predictions can be obtained from the macroscopic data. For all the materials considered here it is found that better predictions are obtained with radial deformation. For the simple deformable-shell model the parameters can be determined from Eqs. (11)–(15). For the deformable-shell model one extra datum is necessary to fix γ. For NaI the measured phonon frequency for the LA phonon at the boundary (1,1,1) was chosen because both the longitudinal modes in this region are particularly sensitive to γ. The value found in this way increases the importance of radial deformation by increasing the ratio of k to k^r from the value of $\frac{1}{3}$ characteristic of pure core-shell interaction. The same procedure could be used for each of the materials considered. However, this same k/k^r ratio has been used for all of them, so that for NaF, NaCl, and NaBr the same macroscopic data have been used in fixing the parameters as were used for the simple deformable model.

It will be seen from Table I that the next-nearest-neighbor forces are increased very significantly when radial deformation is included. Also the parameters are more reasonable. Thus $A(2)$ and $B(2)$ must have opposite signs if the short-range potential function is to decrease as the separation between the next-nearest neighbors increases. From Table I it can be seen that $A(2)$ and $B(2)$ have opposite signs for both the deformable-shell models, but not for the rigid shell.

The dispersion curves for the three models are given in Figs. 3–6.[24–26] The simple deformable-shell model leads to an over-all improvement for both the LA and LO branches for all the materials; however, the predictions are not as good as for a rigid shell in the region of the (0,0,1) boundary. This feature can only be avoided by using model parameters which are inconsistent with the macroscopic data. Some further over-all improvement is found with the deformable-shell model for NaI, NaBr, and NaCl. For instance in NaBr, where the experimental errors in the experimental measurements are known, the χ^2 values for the predicted rigid ion, rigid shell, simple deformable shell, and deformable shells are

[24] W. J. L. Buyers, Phys. Rev. **153**, 923 (1967).
[25] R. E. Schmunk, Bull. Am. Phys. Soc. **12**, 281 (1967).
[26] A. D. B. Woods, B. N. Brockhouse, R. A. Cowley, and W. Cochran, Phys. Rev. **131**, 1025 (1963).

TABLE IV. Percentage changes in the one-phonon cross sections in NaCl as calculated from a rigid-shell model using the three charge distributions (a), (b), and (c).

Scattering vector K	Percentage changes (a)	(b)	(c)	Asymmetry in percentage changes (a)	(b)	(c)
(0,0, 3.8)	0.005	−0.026	−0.02	0.0044	0.024	−0.009
(0,0, 4.2)	0.0006	−0.05	−0.011			
(0,0, 3.6)	0.016	−0.11	−0.067	0.017	0.01	−0.052
(0,0, 4.4)	−0.0009	−0.12	−0.015			
(0,0, 3.4)	−0.031	−0.04	−0.024	−0.041	−0.058	−0.025
(0,0, 4.6)	0.01	0.018	0.001			
(0,0, 3.2)	−0.31	0.14	0.16	−0.35	−0.22	0.19
(0,0, 4.8)	0.038	0.36	−0.028			
(0,0, 3.0)	−0.59	0.13	0.28	−0.53	0.65	0.16
(0,0, 5.0)	−0.06	−0.52	0.12			

118.6, 17.1, 11.7, and 8.9, respectively. However, the increased radial deformation accentuates the discrepancy at the (0,0,1) boundary. For NaF the best predictions are obtained from the simple deformable-shell model.

No significant change in the transverse branches is produced by either deformable-shell model.

The feature in the dispersion curve in the LO (0,0,1) boundary region seems to be an inescapable result of introducing radial deformation with one ion polarizable. It is not likely to result from the different anharmonic contributions to the macroscopic constants and to the measured frequencies in the zero-sound region.[27] Thus for NaI both frequency and elastic constants were measured at 100°K where the difference between the first- and second-sound regions is certainly less than the 20% changes in elastic constants which would be required to remove the boundary feature. Radial deformation gives a similar feature in the boundary curve for KBr but in this material the same behavior is found in the experimental measurements.[10]

The general conclusion drawn from the results of this section on the prediction of dispersion curves from macroscopic constants, particularly for the more polarizable ions where neglect of the distortion of the sodium ion is reasonable, is that classical models incorporating radial deformation represent some important part of the forces between the ions. In the absence of any alternative source of information, the distortions corresponding to the eigenvectors **W** and **R** have therefore been used in Sec. 4 to calculate the form-factor changes when different normal modes are excited in NaCl.

4. FORM-FACTOR CHANGES

A. Form-Factor Changes Calculated from a Rigid-Shell Model

The $\beta(\mathbf{q},\mu\mu',\mathbf{K})$ coefficients which occur in the one-phonon cross sections (Sec. 2) can be calculated for any deformation model from the ionic form-factor changes when the different modes of a specific $\mathbf{q}$ are excited. Thus it can easily be shown that the contribution to the fractional change in form factor when the $(\mathbf{q},j)$ mode is excited is given by

$$\frac{\Delta f(\mathbf{q},j,\mu)}{f(\mu)}=\sum_{\mu'}\beta(\mathbf{q},\mu\mu',\mathbf{K})\cdot\mathbf{U}(\mathbf{q},j,\mu').$$

If this change can be calculated from a model for each pair of acoustic and optic modes of a given $\mathbf{q}$, then as the eigenvectors for the two modes are known, the separate values $\beta(\mathbf{q},\mu\mu,\mathbf{K})$ and $\beta(\mathbf{q},\mu\mu',\mathbf{K})$ can be obtained.

For an undisplaced shell ($\mathbf{W}=0$) the ionic form factor can be written as the sum of the shell and core contributions.

$$f(\mu)=f_c(\mu)+f_s(\mu).$$

When the core-shell displacement is $\mathbf{W}$, the fractional change in the scattering factor is

$$\frac{\Delta f(\mathbf{q},j,\mu)}{f(\mu)}=\frac{f_S(\mu)}{f(\mu)}[\exp(i\mathbf{K}\cdot\mathbf{W})-1].$$

The values of $\Delta f(\mathbf{q},j\mu)/f(\mu)$ are therefore determined by $\mathbf{W}$ and by the charge distribution carried by the shell.

Table III gives the magnitudes of $\beta(\mathbf{q},\mu\mu',\mathbf{K})$ coefficients determined in this way. The values of $\mathbf{W}$ were obtained from the rigid-shell model used in Sec. 3 D. The total charge on the shell was taken as the shell charge (Y) given by the model, and the three sets of results given in Table III are for the following three different shell charge distributions: (a) the 3*s* distribution for Cl^- (James[28]), (b) a thin spherical annulus of charge with a radius of 1.5 A, and (c) the distribution corresponding to the outer Y electrons in the Cl^- electron distribution. The changes in the one-phonon intensities along the (0,0,1) axis corresponding to Table III

[27] R. A. Cowley, Proc. Phys. Soc. (London) **90**, 1127 (1967).

[28] R. W. James, Phil. Mag. **12**, 81 (1931).

TABLE V. Values of the magnitude $\beta(\mathbf{q},\mu\mu',\mathbf{K})$ for NaCl using the radial deformation given by the deformable-shell model and the charge distributions (b) and (c). All quantities are in units of $\pi/10a$ (cation $\mu=1$; anion $\mu=2$).

Scattering vector K	$\beta(\mathbf{q},21,\mathbf{K})$ (b)	$\beta(\mathbf{q},21,\mathbf{K})$ (c)	$\beta(\mathbf{q},22,\mathbf{K})$ (b)	$\beta(\mathbf{q},22,\mathbf{K})$ (c)
(0,0, 3.8)	0.08	−0.055	0	0
(0,0, 4.2)	0.042	0.072	0	0
(0,0, 3.6)	0.18	−0.06	0	0
(0,0, 4.4)	0.13	0.13	0	0
(0,0, 3.4)	0.22	−0.02	0	0
(0,0, 4.6)	0.20	0.13	0	0
(0,0, 3.2)	0.15	0.0077	0	0
(0,0, 4.8)	0.16	0.077	0	0
(0,0, 3.0)	0	0	0	0
(0,0, 5.0)	0	0	0	0

TABLE VI. Percentage changes in the one-phonon cross sections in NaCl from radial deformations for the deformable-shell model using the change distributions (b) and (c).

Scattering vector K	Percentage changes (b)	Percentage changes (c)	Asymmetry in percentage changes (b)	Asymmetry in percentage changes (c)
(0,0, 3.8)	−0.26	0.17	−0.14	0.37
(0,0, 4.2)	−0.12	−0.20		
(0,0, 3.6)	−0.60	0.191	−0.24	0.52
(0,0, 4.4)	−0.36	−0.33		
(0,0, 3.4)	−0.70	0.061	−0.25	0.35
(0,0, 4.6)	−0.45	−0.29		
(0,0, 3.2)	−0.4	−0.021	−0.14	0.11
(0,0, 4.8)	−0.26	−0.13		
(0,0, 3.0)	0	0	0	0
(0,0, 5.0)	0	0		

are given in Table IV. The intensity changes are never more than 1%, and the changes produced at equivalent points ($\mathbf{K}=\mathbf{H}\pm\mathbf{q}$) on either side of the Bragg peak are similar, so that any asymmetry in the cross sections at these points (Table IV) is an order of magnitude less than the measured value.[3] One can conclude that rigid-shell displacements do not adequately represent the ionic distortions that occur.

B. Form-Factor Changes Calculated for a Deformable Shell

For both the simple deformable and the deformable shells, the form-factor changes can be obtained for the core-shell displacements in a similar way to that described in Sec. 4 A. Since the displacement eigenvectors ($\mathbf{U}_j$) and ($\mathbf{W}_j$) are almost identical (5%) with the rigid-shell values, the changes in the one-phonon cross section are essentially the same as those given in Table IV. However, the radial changes now lead to additional form-factor effects which can be computed from the radial eigenvectors $R(k)$. The values of $\beta(\mathbf{q},\mu\mu',\mathbf{K})$ and the percentage changes in the one-phonon cross sections have been estimated using the shell distributions (b) and (c) of Sec. 4 A, and the results are given in Tables V and VI. The radial distortions are due to nearest-neighbor interactions, so that $\beta(\mathbf{q},22,\mathbf{K})$ is always zero. It is clear (Table VI) that the predicted intensity changes are very different for the two charge distributions. Also the $\mathbf{K}$ dependence of $\beta(\mathbf{q},\mu\mu',\mathbf{K})$ for $\mathbf{K}=\mathbf{H}\pm\mathbf{q}$ gives intensity changes at these equivalent points which are not of similar magnitude and opposite sense, and the asymmetries are generally less than the shifts (Table VI). The intensity changes are rather greater than those due to the relative displacement of core and shell, but are still an order of magnitude less than the observed asymmetries. It seems certain that no change in the assumed shell distribution would lead to the required increase.

We therefore conclude that a classical shell model with radial deformation is a useful description of the forces between ions, and may give a reasonable account of the outer electrons deformation. However, it cannot give any account of the total ionic distortions which occur during lattice vibrations. Quantum-mechanical calculations for both metals and ionic crystals are now in progress.